GE Energy

David H. Hinds
Manager, ESBWR

PO Box 780 M/C L60
Wilmington, NC 28402-0780
USA

T 910 675 6363
F 910 362 6363
david.hinds@ge.com

MFN 06-210

Docket No. 52-010

July 5, 2006

U.S. Nuclear Regulatory Commission
Document Control Desk
Washington, D.C. 20555-0001

Subject: **NEDO-33201, Revision 1, "ESBWR Probabilistic Risk Assessment," Section 15**

Enclosure 1 contains the subject partial ESBWR Probabilistic Risk Assessment (PRA) document (Revision 1).

If you have any questions about the information provided here, please let me know.

Sincerely,

Kathy Sedney for

David H. Hinds
Manager, ESBWR

D068

Enclosure:

1. MFN 06-210 – NEDO-33201, Revision 1, "ESBWR Probabilistic Risk Assessment:"
    - Section 15 – Seismic Margins Analysis

cc: WD Beckner USNRC (w/o enclosures)
AE Cubbage USNRC (with enclosures)
LA Dudes USNRC (w/o enclosures)
GB Stramback GE/San Jose (with enclosures)
eDRF 0000-0044-8542

ENCLOSURE 1

MFN 06-210

NEDO-33201, Revision 1, "ESBWR Probabilistic Risk Assessment"

- **Section 15 – Seismic Margins Analysis**

15 SEISMIC MARGINS ANALYSIS

Contents

List of Tables

List of Figures

15 SEISMIC MARGINS ANALYSIS

This section documents the seismic analysis of the ESBWR PRA.

15.1 INTRODUCTION

The seismic risk analysis is performed to assess the impacts of seismic events on the safe operation of the ESBWR plant.

A seismic margins analysis (SMA) is performed for the ESBWR using a modification of the fragility analysis method of Reference 15-1 to calculate high confidence low probability of failure (HCLPF) accelerations for important accident sequences and accident classes.

The analysis shows that the ESBWR plant and equipment are capable of withstanding an earthquake with a magnitude at least two times the safe shutdown earthquake (SSE) with a high confidence of low probability of failure.

The scope of the analysis includes both at-power and shutdown seismic-induced accident scenarios.

15.2 METHODOLOGY

The seismic risk assessment uses a seismic margins analysis (SMA) method based on that of Reference 15-1 to calculate high confidence low probability of failure (HCLPF) accelerations for important accident sequences and accident classes.

The seismic margins approach used in this analysis evaluates the capability of the plant and equipment to withstand an earthquake of 2 times the safe shutdown earthquake (2*SSE). (Reference 15-1)

The analysis involves the following two major steps:

(1) Seismic fragilities

(2) Accident sequence HCLPF analysis

The seismic fragilities of the ESBWR systems, structures, and components are based on generic industry information and ESBWR specific seismic capacity calculations for certain structures.

The MIN-MAX method is used in the determination of functional and accident sequence fragilities. Per the MIN-MAX method, the overall fragility of a group of inputs combined using OR logic (i.e., seismic event tree nodal fault tree) is determined by the lowest (minimum) HCLPF input. Conversely, per the MIN-MAX method, the overall fragility of a group of inputs combined using AND logic (i.e., seismic event tree sequence) is determined by the highest (maximum) HCLPF input.

Both at-power and shutdown seismic-induced accident scenarios are analyzed.

15.3 SEISMIC FRAGILITIES

15.3.1 Overview

This subsection presents seismic capacities for selected structures and components that have been identified as potentially important to the seismic risk analysis of the ESBWR standard plant. The seismic capabilities in terms of seismic fragilities are first estimated, from which the high confidence low probability of failure (HCLPF) capacities are then derived. The HCLPF capacities serve as input to the system analysis following the seismic margins approach.

The peak ground acceleration of the design earthquakes is 0.3g minimum for the Safe Shutdown Earthquake (SSE). Extensive seismic soil-structure interaction analyses of the reactor building and control building complex were performed for a wide range of generic site conditions under a 0.3g SSE and for North Anna Early Site Permit (ESP) site-specific SSE. The analysis results in terms of site-envelope SSE loads are presented in Appendix 3A of the ESBWR DCD Tier 2 Rev. 1 (Reference 15-2). The standard plant designed to these site-envelope seismic loads may result in significant design margins when it is situated at a specific site, particularly a soft soil site. Thus, the seismic capacities estimated from the site-envelope design requirements may be very conservative for certain sites.

For the seismic category I structures and components for which seismic design information is available, the seismic fragilities are evaluated using the factor of safety approach, which is called the Zion method in NUREG/CR-2300, PRA Procedures Guide (Reference 15-3). This approach identifies various conservatisms and associated uncertainties introduced in the seismic design process and provides a probabilistic estimate of the earthquake level required to fail a structure or component in a postulated failure mode by linear extrapolation of the design information supplemented by judgment.

For certain safety-related components such as pumps, valves, and electrical equipment whose design details are not currently available, the generic seismic fragilities recommended in the EPRI ALWR Utility Requirements Document, Appendix A PRA Key Assumptions and Ground rules (Reference 15-4) or other data sources (References 15-5 and 15-6) are used as appropriate. Those generic fragilities were chosen based on a review of prior PRAs and fragility data. They are considered achievable for the ESBWRs with an evolutionary improvement in the seismic capacities of the components designed to a 0.3g SSE minimum.

15.3.2 Fragility Formulation

Seismic fragility of a structure or component is defined herein to be the cumulative conditional probability of its failure as a function of the mean peak ground acceleration (i.e., the average of the peak of the two horizontal components).

The probability model adopted for fragility description is the lognormal distribution. Using the lognormal distribution assumption, an entire family of fragility curves can be fully described in terms of the median ground acceleration and two random variables as:

$$A = A_m \varepsilon_\gamma \varepsilon_\mu \qquad (15.3\text{-}1)$$

Where:

A_m = median peak ground acceleration corresponding to 50% failure probability.

ε_γ = a lognormally distributed random variable accounting for inherent randomness about the median. It is characterized by unit median and logarithmic standard deviation β_γ.

ε_μ = a lognormally distributed random variable accounting for uncertainty in the median value. It is characterized by unit median and logarithmic standard deviation β_μ.

With known values of A, β_γ, and β_μ, the failure probability P_f at acceleration less than m or equal to a given acceleration a can be computed using the following equation for any non-exceedance probability (NEP) level Q.

$$P_f(A \le a|Q) = \phi\left[\frac{1}{\beta_\gamma} In\left(\frac{a}{A_m}\right) + \frac{\beta_\mu}{\beta_\gamma}\phi^{-1}(Q)\right] \quad (15.3\text{-}2)$$

Where φ is the standard Gaussian cumulative distribution function. Figure 15-1 shows a typical family of fragility curves for various NEP levels. The center solid curve represents the median fragility curve at 50% NEP level. The logarithmic standard deviation of the randomness component β_γ determines the curve slope. The logarithmic standard deviation of the uncertainty component β_μ is a measure of the spread from the median curve. The 95th percentile and 5th percentile curves in Figure 15-1 are the upper and lower bounds of the failure probability for a given acceleration, corresponding to 95% and 5% NEP levels, respectively.

When only the point estimate is of interest, which is the case for this analysis, the total variability about the median value is taken to be the square root of the sum of the squares (SRSS) of the randomness and uncertainty components.

$$\beta_c = \sqrt{\beta_\gamma^2 + \beta_\mu^2} \quad (15.3\text{-}3)$$

The fragility curve corresponding to the median value A_m with associated composite logarithmic standard deviation can be computed by the following equation:

$$P_f(A \le a) = \phi\left[\frac{1}{\beta_c}\ln\left(\frac{a}{A_m}\right)\right] \quad (15.3\text{-}4)$$

This composite fragility curve is also called the mean fragility curve and is shown as the dashed curve in Figure 15-1 for illustration. It represents the best estimate fragility description.

In estimating the median ground acceleration capacity and the associated variability, an intermediate variable defined as safety factor F is utilized. The safety factor is related to the median ground acceleration capacity by the following relationship.

$$A_m = FA_d \quad (15.3\text{-}5)$$

Where A_d is the ground acceleration of the reference design earthquake to which the structure or component is designed. A key step in the seismic fragility estimate thus involves the evaluation of the factor of safety associated with the design for each important potential failure mode. The design margins inherent in the component capacity and the dynamic response to the specific acceleration are the two basic considerations. Each of the capacity and response margins involves several variables, and each variable has a median factor of safety and variability

associated with it. The overall factor of safety F is the product of the factor of safety for each variable F_i.

$$F = \prod_i F_i \tag{15.3-6}$$

The overall composite logarithmic standard deviation is SRSS of the composite logarithmic standard deviations in the individual factors of safety.

$$\beta_c = \sqrt{\sum_i \beta_{ci}^2} \tag{15.3-7}$$

Knowing the median peak ground acceleration (A_m) and associated logarithmic standard deviation (β_c); the HCLPF capacity is obtained using the equation below.

$$\text{HCLPF} = A_m \exp(-2.326\beta_c) \tag{15.3-7a}$$

15.3.3 Structural Fragility

The plant structures are divided into two categories according to their function and the degree of integrity required to protect the public during a seismic event. These categories are seismic category I and non-category I. Seismic category I includes those structures whose failure might cause or increase the severity of an accident, which would endanger the public health and safety. The reactor building and control building structures are in this category. The non-category I structures are those structures which are important to reactor operation, but are not essential for preventing an accident which would endanger the public health and safety, and are not essential for the mitigation of the consequences of these accidents. One example is the turbine building structure.

For the purpose of this study, structures are considered to fail functionally when inelastic deformations of the structure under seismic load increase to the extent that the operability of the safety-related components attached to the structure cannot be assured. The ductility limits chosen for structures are estimated as corresponding to the onset of significant structural damage. For many potential modes of failure, this is believed to represent a conservative bound on the level of inelastic structural deformation that might interfere with the function of the system housed within the structure.

The potential of seismic-induced soil failure such as liquefaction, differential settlement, or slope instability is highly site dependent and cannot be assessed for generic site conditions. It is assumed in this analysis that there is no soil failure potential in the range of ground motions considered.

Building-to-building impact due to differential building displacements under strong earthquakes is deemed not credible since a sufficient distance to avoid impact separates adjacent buildings. Differential building displacements of sufficient magnitude could, however, potentially result in damage to interconnecting piping, depending on system configuration and sliding resistance of building foundation. Detailed evaluation of seismic capacities of interconnecting systems against differential building displacement cannot be made due to lack of design details and specific site conditions. It is assumed that the mode of failure due to differential building displacement has a capacity no less than the generic piping fragility of 3g (Table 15-1).

15.3.3.1 Reactor Building Complex Structures

Detailed fragility evaluations were made for the following structures in the reactor building (RB) and fuel building (FB) complex. The RB and FB share the same basement and are fully integrated. The term "reactor building" when mentioned hereafter also includes the structures of the fuel building. As for the containment structure, it is enclosed by and integrated into the RB.

- Building shear walls
- Containment wall (upper drywell and wetwell)
- RPV pedestal (same as lower drywell wall)
- RPV support brackets

Those structures were evaluated according to the approach outlined previously and using various safety factors as presented below.

The factor of safety for a structure against a specific failure mode is the product of the capacity factor F_c and structural response factor F_{rs};

$$F = F_c F_{rs} \tag{15.3-8}$$

The individual factors, the capacity factor and the response factor, are discussed in the following subsections.

15.3.3.1.1 Capacity Factor (F_c)

The capacity factor represents the capability of a structure to withstand seismic excitation in excess of the design earthquake. This factor is composed of two parts:

$$F_c = F_s F_u \tag{15.3-9}$$

Where:

F_s = the ultimate structural strength margin above the design SSE load, and

F_u = the inelastic energy absorption factor accounting for additional capacity of the structure to undergo inelastic deformations beyond yield.

The capacity estimated by this approach is the elastic capacity equivalent to the actual nonlinear behavior under strong motion earthquakes.

Strength Factor (Fs)

The strength factor associated with seismic load can be calculated using the following equation.

$$F_s = \frac{P_u - P_n}{P_s} \tag{15.3-10}$$

Where:

P_u = the actual ultimate strength,

P_n = the normal operating loads, and

P_s = the design SSE load.

The earthquake-resistant structural elements of the reactor building are reinforced concrete shear walls that are integrated with the reinforced concrete cylindrical containment through concrete floor slabs. The specified compressive strength of concrete is 34.5 MPa for the building and 27.5 MPa for the mat. The specified yield strength of reinforcing steel of ASTM A615, Grade 60 is 414 MPa. These are design values; the actual material strengths are higher.

Concrete compressive strength used for design is normally specified as a value at a specific time after mixing (28 or 90 days). This value is verified by laboratory testing of mix samples. The strength must meet specified values, allowing a finite number of failures per number of trials. There are two major factors that affect the actual strength:

a. To meet the design specifications, the contractor attempts to create a mix that has an "average" strength somewhat above the design strength, and

b. As concrete ages, it increases in strength.

Taking those two elements into consideration, the actual compressive strength of aged concrete is commonly 1.3 times the design strength (Reference 15-7). The total logarithmic standard deviation about the median strength is about 0.13.

According to the same reference, the ratio of the median yield strength to the specified strength of reinforcing steel is taken to be 1.2 with logarithmic standard deviation of 0.12.

The median yield strength of steel plates is typically 1.25 times the code specified strength with logarithmic standard deviation of 0.14 (References 15-7 and 15-8).

The reactor building shear wall is chosen as an example for the discussion of the strength factor evaluation. For reinforced concrete shear walls the ultimate shear strength can be computed using the following equation (Reference 15-9).

$$v_u = v_c + v_s$$

$$= 8.3\sqrt{f_c} - 3.4\sqrt{f'_c}\left(\frac{h}{w} - \frac{1}{2}\right) + \frac{N}{4wt} + \rho_{se} f_y \qquad (15.3\text{-}11)$$

Where:

v_c = shear strength provided by concrete

v_s = shear strength provided by reinforcing steel

f'_c = concrete compressive strength

h = wall height

w = wall length

N = bearing load

f_y = yield strength of reinforcing steel

t = wall thickness

ρ_{se} = $A\rho_v + B\rho_h$

ρ_h = horizontal steel reinforcement ratio

ρ_v = vertical steel reinforcement ratio

A & B = constants depending on h/w:

	A	B
h/w< 0.5	1	0
0.5 ≤ h/w< 1.0	2(1-h/w)	(2h/w-1)
1.0 < h/w	0	1

In computing ultimate shear strength with this equation, the median material strengths of the concrete and reinforcing steel defined above are used and the wall bearing load is conservatively neglected.

The strength factor F_s is then calculated using Equation 15.3-10 for each of the levels of the reactor building shear walls. The normal operating loads do not result in lateral force and horizontal loads induced by SRV actuations are found to be negligible compared to the SSE-induced horizontal loads. Therefore, the strength factor is the ratio of the median shear strength to the design SSE shear. The lowest strength factor is found to be 2.00. The associated logarithmic standard deviation is calculated to be 0.09 using the second moment approximation (Reference 15-9) accounting for both concrete and reinforcing steel material strength variabilities. There is also an uncertainty associated with Equation 15.3-11 since it is an approximate model fit to data. The modeling uncertainty is 0.15 expressed in terms of logarithmic standard deviation (Reference 15-9). The total composite logarithmic standard deviation in the median strength factor is 0.17, which is the SRSS value of 0.09 for the material strength uncertainty and 0.15 for the equation uncertainty.

Inelastic Energy Absorption Factor (F_u)

The inelastic energy absorption factor (F_u) accounts for the fact that an earthquake represents a limited energy source and many structures are capable of absorbing substantial amounts of energy beyond yield without loss of function. The parameter commonly used to measure the energy absorption capacity in the inelastic range is the ductility ratio, μ. It is defined as the ratio of the maximum displacement to the displacement at yield. Newmark, Reference 15-10, has shown that in the amplified acceleration range (approximately 2 to 8 Hz) the inelastic energy absorption factor F_u can be estimated by

$$F_u = \varepsilon\sqrt{2\mu - 1} \qquad (15.3\text{-}12)$$

Where ε is an error variable to account for the uncertainty associated with the use of this equation. This error variable is assumed to be lognormally distributed with a median of unity and a logarithmic standard deviation ranging from 0.02 to 0.1 (Reference 15-11). For rigid structures (fundamental frequency above 20 Hz), the following equation given by Reference 15-11 may be used.

$$F_u = \varepsilon\mu^{0.13} \qquad (15.3\text{-}13)$$

Again, ε is an error variable of unit median and logarithmic standard deviation ranging from 0.02 to 0.1. For intermediate frequencies, the F_u factor can be interpolated from Eqs. 15.3-12 and 15.3-13.

According to Reference 15-7, the system ductility ratio for reinforced concrete shear walls failing in shear is 2.5. The integrated building/containment system responds in multiple modes with predominant modes up to 10 Hz. The corresponding inelastic energy absorption factor is thus about 2.0 according to Equation 15.3-12. The associated logarithmic standard deviation is 0.25 (Reference 15-7). Flexural failures tend to be more ductile than shear failures. A ductility ratio of 4.0 is estimated and the corresponding F_u is 2.65 with logarithmic standard deviation of 0.25.

Steel structures are typically more ductile than concrete structures. When local buckling is prevented, the allowable ductility ratio is 5 (Reference 15-12) for which the corresponding F_u is 3. The F_u factor is taken as unity when the failure mode is of a brittle type such as buckling or failure of high strength anchor bolts.

15.3.3.1.2 Structural Response Factor (F_{rs})

The structural response factor (F_{rs}) consists of a number of factors or parameters introduced in the calculation of structural response in the seismic dynamic analysis. Response calculations performed in the design analysis utilized conservative deterministic parameters. The actual response may differ significantly from the calculated response for a given peak ground acceleration level since many of these parameters are random. The structural response factor is evaluated as the product of the following factors that are considered to have the most influence on the structural response.

$$F_{rs} = F_{sa}F_dF_{ssi}F_mF_{mc}F_{ecc} \qquad (15.3\text{-}14)$$

Where:

- F_{sa} = spectral shape factor accounting for the margin of the design ground response spectra with respect to the median centered spectra,
- F_d = damping factor accounting for the variability in response due to difference in expected damping at failure and damping used in the analysis,
- F_{ssi} = soil-structure interaction factor accounting for the variability associated with SSI effects on structural response,
- F_m = structural modeling factor accounting for the variability in response due to modeling assumptions,
- F_{mc} = modal response combination factor accounting for the variability in response due to the method used in combining modal responses,
- F_{ecc} = earthquake component combination factor accounting for the variability in response due to the method used in combining the earthquake components.

Spectral Shape Factor (F_{sa})

The ground response spectrum considered in the seismic design is taken from both Regulatory Guide (RG) 1.60 site-independent ground spectra and the North Anna ESP site-specific ground spectra. In accordance with the soil-structure interaction analysis performed and described in Appendix 3A, generic sites with 0.3g RG 1.60 input typically higher results in higher structural responses than North Anna ESP conditions for building structures including the containment. Therefore, the spectral shape factor discussed below is derived relative to RG 1.60 ground spectra, normalized to the design ground acceleration. To facilitate dynamic analysis using the time history method, artificial acceleration time histories of three directional components were generated so that the resulting spectra envelop the design spectra for the damping ratios of interest.

For the purpose of seismic risk assessment, the median ground spectrum given in NUREG/CR-0098 (Reference 15-13) is considered to be the realistic input ground motion definition. The differences between the design spectra and median spectra are the margins in the ground motion input.

The spectral shape factor (F_{sa}) is defined to be the ratio of the amplification factor of the design spectrum to that of the median spectrum at the same frequency and damping level.

$$F_{sa} = AF_d / AF_m \qquad (15.3\text{-}15)$$

In constructing the median spectrum, the competent soil condition is conservatively assumed since it results in higher maximum ground velocity and displacement amplitudes than the rock condition for the same maximum ground acceleration. The design spectrum and median spectrum are compared at the 5% damping level for the maximum ground acceleration of 1g. The average spectral shape factors in representative frequency ranges are approximately

Frequency Range (Hz)	Average F_{sa}
2 to 10	1.34
10 to 20	1.20
20 to 33	1.07
Above 33	1.00

The logarithmic standard deviation in the spectral shape factor is the variability in the median spectra, which is 0.2 according to Reference 15-4. No variability exists for frequencies above 33 Hz.

Damping Factor (F_d)

The SSE loads were calculated using the SSE damping ratios specified in RG 1.61. The RG 1.61 damping values are considered to be quite conservative, particularly at response levels near failure. More realistic damping values are specified in Reference 15-13.

For reinforced concrete structures the damping ratio considered in the SSE analysis is 7%. The realistic values at or near yield range from 7 to 10% (Reference 15-13). The upper bound value is considered to be the median and the lower bound corresponds to the 84th percentile level.

The RG 1.60 design ground spectra are used to evaluate the margin in response due to difference in actual damping at failure and design damping. The damping factor F_d can be calculated to be

the ratio of the amplification factor at design damping (AF_{dd}) to the amplification factor at median damping (AF_{md}) at the same frequency.

$$F_d = AF_{dd} / AF_{md} \qquad 15.3\text{-}16)$$

The associated logarithmic standard deviation can be calculated to be the natural log of the ratio of the amplification factor at 84th percentile damping (AF_{bd}) to the amplification factor at median damping (AF_{md}) at the same

$$ßc = \ln (AF_{bd} / AF_{md}) \qquad (15.3\text{-}17)$$

For reinforced concrete structures the average damping factors and associated logarithmic standard deviations in representative frequency ranges are approximately

Frequency Range (Hz)	Average F_d	Average $ß_c$
2 to 10	1.19	0.18
10 to 20	1.12	0.11
20 to 33	1.02	0.02
Above 33	1.00	0.0

Soil-Structure Interaction Factor (F_{ssi})

The design seismic loads were established to be the site-envelope loads calculated by the SSI analyses. The site-envelope loads may have margins for a given site. The margin may be substantial if the specific site is a soft soil site. Since the ESBWR standard plant is designed for generic site conditions, no credit is taken for site margins. Thus, the factor is taken as 1.0. The associated logarithmic standard F_{SSI} deviation is estimated to be 0.1.

Modeling Factor (F_m)

The reactor building complex structural model considered in the seismic design analysis is a multi-degree-of-freedom system constructed according to common modeling techniques and the Standard Review Plan (SRP) requirements in terms of number of degrees of freedom and subsystem decoupling. The model is thus considered to be the best estimate and the resulting dynamic characteristics are the median centered. The modeling factor is thus unity. A relatively large logarithmic standard deviation of 0.15 is estimated to account for the complexity of the integrated reactor building and the containment design.

Modal Response Combination Factor (F_{mc})

The analysis method used in the seismic response analysis is the time history method solved by direct integrations. The phasing between individual modal responses is known and the total response is the algebraic sum of all modes of interest. The maximum response is thus precise and the modal response combination factor (F_{mc}) is unity. The associated uncertainties should be less than the uncertainties associated with the response spectrum method, in which the maximum modal responses are combined by the SRSS method. Therefore, a relatively small logarithmic standard deviation of 0.05 is estimated.

Earthquake Component Combination Factor (F_{ecc})

The effects of multi-directional earthquake excitation on structural response depend on the geometry, dynamic response characteristics, and relative magnitudes of the two horizontal and the vertical earthquake components. The design method is SRSS or 100-40-40. Either method is considered to result in a median-centered response. The earthquake component combination factor is 1.0.

The reactor building walls are designed to resist in-plane loads. The walls mainly respond to the horizontal motion parallel to the walls. The vertical loads on the walls due to the vertical excitation are typically less significant in contributing to the total stresses and there is an equal probability of acting upward or downward. The earthquake component combination effect on the wall design is thus not significant and a small logarithmic standard deviation of 0.05 is estimated.

Other major structures inside the reactor building such as the containment and the pedestal are cylindrical structures. The responses to the three orthogonal excitation components are essentially uncoupled. The logarithmic standard deviation is estimated to be 0.05.

15.3.3.1.3 Fragility Results for Reactor Building Complex

The results of the fragility analysis for the identified reactor building failure modes are summarized in Tables 15-2 through 15-5. The overall safety factor is the product of the individual factors. The total logarithmic standard deviation is the SRSS value of the individual logarithmic standard deviations. The seismic fragility, in terms of median ground acceleration, is the product of the overall factor and the SSE design ground acceleration of 0.3 g. The HCLPF calculated in accordance with the seismic margins method of Reference 15-1 for each failure mode is summarized at the bottom of each of the tables.

15.3.3.2 Control Building Structure

The control building fragility is evaluated using the same procedure described above for the reactor building. The controlling mode of failure is flexural of shear walls. Table 15-6 shows the margin in each of the strength and response factors. The resulting fragility is 4.1 g median peak ground acceleration with a logarithmic standard deviation of 0.44.

15.3.4 Component Fragility

The ESBWR generic components of interest for this seismic risk analysis are the following:

- Shroud support
- CRD guide tubes
- CRD housings
- Fuel assemblies
- Cable trays
- Air-operated valves
- Heat exchangers

- Off-site Power (transformers and ceramic insulators)
- Batteries and battery racks
- Electric equipment (chatter failure mode)
- Switchgear/Motor control centers
- Transformers (480V)
- Motor-driven pumps
- Diesel-driven pumps
- Small tanks (e.g., standby liquid control tank)
- Motor-operated valves
- Safety relief, manual, and check valves
- Hydraulic control units
- Heating, ventilation, and air conditioning ducting
- Air handling units/room air conditioners
- Piping

The shroud support, CRD guide tubes, CRD housing, and fuel assembly fragilities are calculated in a like manner as discussed above in Section 15.3.3. These calculations are summarized in Tables 15-7 through 15-10.

Seismic fragilities for the other component items are obtained from generic sources, as discussed in Section 15.3.1.

15.3.5 Fragility Summary

The structural and component seismic fragilities, and corresponding HCLPF values, are summarized in Table 15-1. These are the same as the ones considered in the ABWR SSAR based on past experience and ALWR recommendations.

15.4 ACCIDENT SEQUENCE HCLPF ANALYSIS

An event tree structure is used in the ESBWR seismic margin analyses to illustrate the accident sequences analyzed in the analysis. This event tree structure is shown in Figure 15-2.

The seismic event tree is used to identify those structures and components requiring seismic capacity analysis (refer to Section 15.3), and to identify the HCLPFs of individual seismic-induced accident sequences.

If a system, S, (or sequence) contains two components (A, B) combined with OR logic, the failure of any component will fail the system (S = A + B), and the cumulative fragility distribution of the system is governed by the fragility distribution of the weakest component. This principle is applied to the system fault trees, which generally are comprised of OR gates.

If two elements operate in AND logic, only the failure of both components will fail the system (S = A * B), and the cumulative fragility distribution of the system is governed by the fragility distribution of the most seismically rugged component. This principle is applied to accident sequences, which are composed of AND elements.

The scope of this analysis includes both at-power and shutdown seismic-induced accident scenarios. The seismic accident analysis for the at-power condition is discussed below in Section 15.4.1, and the analysis for the shutdown condition is discussed in Section 15.4.2.

15.4.1 Full Power Analysis

15.4.1.1 Full Power Seismic Event Tree

The seismic event tree is shown in Figure 15-2. The HCLPF fragility information input into each event tree node is obtained from the fragility analysis summarized in Section 15.3. The HCLPF inputs as a function of event tree node are summarized in Table 15-11.

The event tree begins with the spectrum of seismic events, considers whether or not seismic-induced structural failure (node SI) occurs, and whether or not emergency DC power is lost. Loss of either structural integrity or DC power results in core damage. Thus, all remaining accident sequences in Figure 15-2 are for cases of no structural failure and DC power available.

The success or failure of emergency DC power (node DC) is evaluated in Figure 15-2 to account for support system dependencies. Failure of all DC power results in a high-pressure core melt since all control is lost, the isolation condensers fail, and the reactor cannot be depressurized.

In event of successful emergency DC, the next node questions whether or not seismic-induced failure to scram (node SCRAM) occurs. In the event of an ATWS, sufficient safety relief valves must open to prevent RPV failure due to overpressure. Failure of a sufficient number of safety relief valves to open is assumed to lead to a core damage condition due to the severe potential impact on boron injection effectiveness.

If the SRVs function properly, the next node questions the actuation of the Standby Liquid Control (SLCS) system. Seismic-induced failure of SLCS leads to a core damage condition.

For sequences with failure to scram (SCRAM node failure) but successful SLCS initiation, once the reactor is subcritical and all SRVs are closed, heat removal is achieved through the Isolation Condensers. No credit is given to the actuation of the Passive Containment Cooling system

because of the impact on boron injection effectiveness. Failure of the Isolation Condenser after SLCS leads to a core damage condition.

To extend Isolation Condensers performance well beyond 24 hours, communication between the isolation condenser pools and the PCCS pools must be established. As an alternative to this action, water from a fire protection diesel driven pump may be aligned.

The successful condition of the Scram function (SCRAM node success) leads to another group of sequences. In this group, actuation of the SRVs is also required for initial pressure control. Additional RPV depressurization using the DPVs is required to allow low pressure injection. These valves discharge to the drywell and after their actuation, the Gravity Driven Cooling system (GDCS) is required to provide water to keep the core covered and to compensate for the water losses due to steam discharge to the drywell. Failure of either function will lead to core damage.

Heat removal from the drywell will be achieved through the actuation of the Passive Containment Cooling system (PCCS), a fully passive system that condenses the steam and drives the water back to the GDCS pools. In order to ensure that non-condensable gases cannot prevent steam circulation through PCCS heat exchangers it is necessary that the non-condensables be directed to the wetwell. In order to facilitate this process, wetwell pressure must be lower than drywell pressure. All vacuum breakers that separate the drywell from the wetwell must all be closed to prevent equalizing the wetwell and drywell pressure. It is considered that the failure of one vacuum breaker would prevent the successful operation of the PCCS and consequently would lead to core damage.

Whether heat removal is initially provided by either the isolation condensers (ATWS sequences) or the Passive Containment Cooling System (non-ATWS sequences), long term heat removal success requires that the isolation condensers pool be communicated with the PCCS pools. As an alternative to this action, water from a fire protection diesel driven pump may be aligned.

15.4.1.2 System Analysis

The seismic fault trees contain only those components that might be subject to seismic failure. One of the important ground rules of the seismic margin analysis is that all like components in a system always fail together.

The passive safety systems credited in the analysis have just a few active components (valves), all with automatic actuation and none with reliance on human action that might represent a single failure dominating the overall system reliability. Human actions are required only in the long term and as such, given the low likelihood of failure for operator actions with very long allowable time windows, human action errors do not dominate system failure. As such, random failures are assumed to be non-significant contributors to seismic risk (consistent with past industry seismic studies) and are not explicitly included in the analysis.

Structure failures judged to contribute to seismic core damage are shown on Figure 15-3. In this analysis, any one or more of these structural failures are assumed to result in core damage. The structures having the lowest seismic capacity are the reactor building and control building.

Only passive safety systems are credited in the seismic event tree. The passive concept means that these systems do not require AC power supply for their actuation. However, DC power supply is required for a number of functions in those systems. The PCCS system is the only fully

passive system. These systems require that depressurization valves actuate as well as the Gravity Driven System, and both systems have some dependency on DC power. As such, the DC power supply is considered separately in the seismic event tree. The most critical components in the DC system are the batteries and cable trays that distribute cables associated with DC distribution. Motor control centers are also included, representing the panels that distribute DC and vital AC power to different loads. The seismic fault tree for DC power is shown on Figure 15-4.

The reactor protection system, control rod drive system, and alternate rod insertion system are not modeled because the failure of control rods to insert is dominated by the relatively low seismic fragility of the fuel assemblies, control rod guide tubes, and housings. The seismic fault tree for reactivity control is shown on Figure 15-5. The fuel assemblies are the most fragile component.

The seismic fault tree for safety relief valves, Figure 15-6, models the possible failures of the SRVs themselves. The same is true for the depressurization valves and vacuum breakers (Figures 15-9 and 15-11).

The seismic fault tree for the standby liquid control system is shown on Figure 15-7. Failure of the standby liquid control system is dominated by failure of two components: the squib valves and boron supply tanks. The failure of piping, check valves and motor operated valves is also included in the fault tree.

The seismic fault tree for the isolation condensers is shown in Figure 15-8. Heat exchanger failure is the most significant seismic-induced component failure, failures of nitrogen operated and motor operated valves and the piping are also included.

The gravity driven cooling system is a passive system and the seismic fault tree for this system, Figure 15-10, includes the failure of the squib and check valves, as well as the piping.

The passive containment cooling system is a fully passive system with no active components. The seismic fault tree for PCCS is shown in Figure 15-12; it includes failure of heat exchangers and failure of piping.

Communication between the upper pools requires only the opening of valves. The seismic fault tree for this function is shown in Figure 15-13.

The firewater diesel-driven pump is designed to supply water to the upper pools. The seismic fault tree for this function is shown in Figure 15-14.

15.4.2 Shutdown Analysis

The seismic shutdown analysis uses the same seismic margins approach, as well as many of the risk model elements used in the full power seismic analysis.

The HCLPF nodal fault trees used for the shutdown seismic analysis are the same as those used in the full power seismic analysis, with the exception of the structural failure node.

The earthquake-induced initiating event assumed in the accident sequence analysis is Loss of Preferred Power (LOPP). Scenarios with structural failures are modeled as leading directly to core damage.

Three shutdown seismic event trees are developed to differentiate the major plant operation modes during shutdown conditions. The following three shutdown modes are addressed (consistent with the other external events shutdown analyses): Mode 5, Mode 6-Unflooded, and Mode 6-Flooded.

15.4.2.1 Shutdown Seismic Event Tree

The shutdown seismic event trees are provided in Figures 15-16 through 15-18.

Mode 5 (Cold Shutdown)

The Mode 5 shutdown seismic event tree is shown in Figure 15-16. As discussed previously, the event tree assumes a LOPP condition.

The first node of the tree, SIS, models seismic-induced failures of the containment building, reactor building, control building, RPV pedestal or supports, fuel assemblies or shroud support. Failure of this node is modeled as leading directly to core damage.

The second node of the tree, DC, models seismic-induced failure of emergency DC power. As shown in Figure 15-2, this node models failure of the batteries, motor control centers or cable trays.

Success of the Isolation Condenser, represented by the IC node, guarantees short-term and long-term residual heat removal, even in the event of DC power failure. Failure of both IC and DC leads directly to core damage.

If the isolation condenser function fails but DC power is available, RPV pressure will increase and lead to the actuation of the safety valves, modeled by the SRV node. Sequences with success at the SRV node continue to the node representing fire protection system water injection into the RPV (FPW).

If the SRV function fails, RPV depressurization can be completed using the DPVs. Failure of both SRV and DPV leads directly to core damage.

Following successful RPV depressurization at the DPV node, actuation of the Gravity Driven Cooling System (GDCS node) is next questioned to supply water inventory to maintain the core covered and to compensate for water inventory losses due to steam discharge to the drywell.

For sequences in which the SRVs have failed but successful DPVs, the fire protection system (FPW) can be used as an alternative RPV injection method if GDCS fails.

Long term heat removal, both for successful GDCS or FPW scenarios, requires operation of the PCCS. PCCS is a completely passive system that condenses the steam and returns the condensate to the GDCS pools. In order to ensure that non-condensable gases prevent steam circulation through PCCS heat exchangers, it is necessary that the non-condensables be directed to the wetwell. To facilitate this process, wetwell pressure must be lower than drywell pressure . All vacuum breakers (VB node) that separate the drywell from the wetwell must be closed to prevent equalizing the wetwell and drywell pressure.

Finally, the PI node models failure of the valve allowing communication between the upper pools.

Mode 6 (Unflooded)

The Mode 6-Unflooded shutdown seismic event tree is shown in Figure 15-17. As discussed previously, the event tree assumes a LOPP condition.

The two first nodes of the tree, SIS and DC, are the same as in the Mode 5 tree. Failure of either leads directly to core damage.

Long term cooling in this operation mode would be guaranteed by the actuation of the Fire Protection Water System modeled in the FPW node, or as an alternative, the Gravity Driven Cooling System (GDCS node).

Mode 6 (Flooded)

In this mode of operation, the cavity is flooded and the reactor vessel is open. If an earthquake occurred during this mode, no system would have to be actuated to guarantee long term cooling; only structural integrity would have to be maintained.

The Mode 6-Flooded shutdown seismic event tree, shown in Figure 15-18, includes only one node (SIS) that models the maintenance of structural integrity.

15.4.2.2 System Analysis

The HCLPF nodal fault trees used for the shutdown seismic analysis are the same as those used in the full power seismic analysis, with the exception of the structural failure node. The structural failure nodal fault tree (SIS), refer to Figure 15-15, for the shutdown seismic event tree is developed to include the structural failures included in the full power SI nodal fault tree, as well as the structural elements related to reactivity control.

15.5 RESULTS

The results of the SMA HCLPF accident sequence analysis are shown on Figures 15-2, 15-16, 15-17 and 15-18, and in Tables 15-13 and 15-14. As can be seen, no accident sequence has a HCLPF lower than 0.60 g (i.e., 2 x SSE). As such, the ESBWR plant and equipment are shown to be capable of withstanding an earthquake with a magnitude at least two times the safe shutdown earthquake (SSE).

15.6 INSIGHTS

The ESBWR seismic margins HCLPF accident sequence analysis highlights the following key insights regarding the seismic capability of the ESBWR:

(1) The ESBWR is inherently capable of safe shutdown in response to strong magnitude earthquakes.

(2) The most significant HCLPF sequences (both 0.62g HCLPF) are seismic-induced loss of DC power and seismic-induced ATWS due to seismic-induced failure of the fuel channels and seismic-induced failure of the SLC tank.

15.7 CONCLUSIONS

The ESBWR is inherently capable of safe shutdown in response to strong magnitude earthquakes. The analysis shows that the ESBWR plant and equipment are capable of withstanding an earthquake of a magnitude at least two times the safe shutdown earthquake (SSE) with a high confidence of low probability of failure.

15.8 REFERENCES

15-1 R.P. Kennedy, et al., *Assessment of Seismic Margin Calculation Methods*, NUREG/CR-5270, Lawrence Livermore National Laboratory, March 1989.

15-2 ESBWR Design Control Document, 26A6642 Rev. 01.

15-3 *PRA Procedures Guide*, NUREG/CR-2300, January 1983.

15-4 *ALWR Utility Requirements Document, Volume II, Chapter 1, Appendix A PRA Key Assumptions and Groundrules,* EPRI, October 1988.

15-5 Harrison, S. W., Esfandiari, S., Pandya, D., and Ahmed, R., *Seismic Fragility Curves for Evaluation of Generic Electrical Conduit Supports, to be presented in the ASME PVP Annual Meetings*, Honolulu, Hawaii, July 22-24, 1989.

15-6 Campbell, R. D., Ravindra, M. K., and Bhatia, A., *Compilation of Fragility Information from Available Probabilistic Risk Assessments*, LLNL, September 1985.

15-7 *Report on Quantification of Uncertainties, Report of Seismic Analysis Main Committee*, ASCE, March 15 1983.

15-8 *Severe Accident Risk Assessment—Limerick Generating Station*, NUS Report, April 1983.

15-9 *Handbook of Nuclear Power Plant Seismic Fragilities, Seismic Safety Margins Research Program*, NUREG/CR-3558, June 1985.

15-10 Newmark, N. M., *Inelastic Design of Nuclear Reactor Structures and Its Implication on Design of Critical Equipment*, SMIRT Paper K4/1, 1977 SMIRT Conference, San Francisco, 1978.

15-11 Kennedy, R. P., and Ravindra, M. K., *Seismic Fragilities for Nuclear Power Plant Risk Studies, Nuclear Engineering and Design*, PP47-68, (79) 1984.

15-12 *Structural Analysis and Design of Nuclear Plant Facilities, Manual and Reports on Engineering Practice*, No. 58, ASCE, 1980.

15-13 *Development of Criteria for Seismic Review of Selected Nuclear Power Plants*, NUREG/CR-0098, May 1978.

Table 15-1
Seismic Capacity Summary

Structure/Component	Failure Mode	Capacity[1] A_m (g)	Fragility Combined[2] Uncertainty	HCLPF (g)
Reactor Building	Shear	1.9	0.45	0.67
Containment	Shear	3.89	0.44	1.40
RPV Pedestal	Shear	2.86	0.44	1.03
RPV support brackets	Support	3.64	0.33	1.69
Control building	Flexural	4.12	0.44	1.48
Shroud support	Buckling	2.0	0.36	0.87
CRD guide tubes	Buckling	1.8	0.36	0.78
CRD housing	Plastic yielding	3.5	0.46	1.20
Fuel Assemblies	Channel deflection	1.4	0.35	0.62
Hydraulic Control Unit	LOF	2.0	0.50	0.63
Cable trays	Support	3.0	0.60	0.74
Air-operated valves	Stem binding/Air line	3.0	0.60	0.74
Heat Exchanger	Anchorage	2.0	0.45	0.70
Off-site power	Ceramic insulators	0.3	0.55	0.08
Batteries and battery racks	Anchorage/LOF	3.3	0.46	1.13
Electric equipment (chatter):				
• function req'd during event	Relay chattering[3]	N/A	N/A	N/A
• function req'd after event	Relay chattering[3]	2.0	0.50	0.63
Switchgear/Motor control centers	Functional/Structural	1.8	0.46	0.62
Transformers	Functional/Structural	1.8	0.46	0.62
Motor-driven pumps	Anchorage/Impeller deflection	1.8	0.46	0.62
Small tanks	Anchorage	1.8	0.46	0.62
Motor-operated valves	Operator distortion	3.0	0.60	0.74
Safety relief & check valves	Internal damage	3.0	0.60	0.74
Manual valves	Internal damage	3.6	0.60	0.89
HVAC ducting	Support	3.0	0.60	0.74
Air handling units/Room A.C.	Blade rubbing	2.0	0.50	0.63
Piping	Support	3.0	0.60	0.74
Diesel-driven pumps	Support	1.8	0.46	0.62

Notes to Table 15-1:

(1) Capacities are in terms of median peak ground acceleration.

(2) Combined uncertainties are composite logarithmic standard deviations of uncertainty and randomness

(3) The potential for relay chatter was treated in the following manner. Only the scram safety function is required during a seismic event. This function is fail-safe, so relay chatter would cause a safe state failure (scram) even if relays were employed. For the ESBWR, the scram actuating devices are solid state power switches with no failure mode similar to relay chatter. The scram function is supplemented by an alternate scram method (energizing the air header dump valves) to provide diversity. This method uses relay actuation, but no credit was taken for this capability in the seismic analysis. Therefore, there is no potential for relay chatter to prevent safety actions during a seismic event.

Switchgear and motor control centers do include relays whose failure could prevent safety actions after the seismic event. It was assumed that the indicated capacity of this equipment (1.8) was more representative than the specific relay chatter value (2.0) since switchgear and motor control centers are normally qualified with the auxiliary relays in place. Also, the type of auxiliary relays used tends to be the most rugged of relay types and would have a capacity above 2.0. The multiplexer output devices for GDCS and RWCU/SDC operation have been assumed to be solid state devices (rather than relays), so the relay chatter failure mode does not apply.

Table 15-2

Seismic Fragility for Reactor Building Shear Walls

Component:		Shear Walls		
Failure Mode:		Flexural		
Factor of Safety			**Median Value**	**β_c**
F_c	F_s	strength margin	2.00	0.17
	F_u	inelastic energy absorption	2.00	0.25
F_{rs}	F_{sa}	spectral shape margin	1.34	0.20
	F_d	damping margin	1.19	0.18
	F_{ssi}	soil-structure interaction	1.00	0.10
	F_m	modeling factor	1.00	0.15
	F_{mc}	modal response combination	1.00	0.05
	F_{ecc}	earthquake component combination	1.00	0.05
Overall Factor of Safety (F) and Composite Logarithmic Standard Deviation (β_c):			**6.38**	**0.45**

A_d = Ground Acceleration of the Reference Design Earthquake = 0.3 g

A_m = Median Peak Ground Acceleration = F * A_d = 6.38 * 0.3 = 1.90 g

HCLPF = $A_m \exp(-2.326 * \beta_c)$ = 0.67 g

Table 15-3

Seismic Fragility for Containment Wall

Component:		Containment Lower Wall		
Failure Mode:		Shear		
Factor of Safety			**Median Value**	**$ß_c$**
F_c	F_s	strength margin	4.06	0.15
	F_u	inelastic energy absorption	2.00	0.25
F_{rs}	F_{sa}	spectral shape margin	1.34	0.20
	F_d	damping margin	1.19	0.18
	F_{ssi}	soil-structure interaction	1.00	0.10
	F_m	modeling factor	1.00	0.15
	F_{mc}	modal response combination	1.00	0.05
	F_{ecc}	earthquake component combination	1.00	0.05
Overall Factor of Safety (F) and Composite Logarithmic Standard Deviation ($ß_c$):			**12.95**	**0.44**

A_d = Ground Acceleration of the Reference Design Earthquake = 0.3 g

A_m = Median Peak Ground Acceleration = F * A_d = 12.95 * 0.3 = 3.89 g

HCLPF = A_m * exp (–2.326 * β_c) = 1.40 g

Table 15-4

Seismic Fragility for RPV Pedestal

Component:		RPV Pedestal		
Failure Mode:		Shear		
Factor of Safety			**Median Value**	**β_c**
F_c	F_s	strength margin	3.26	0.14
	F_u	inelastic energy absorption	2.00	0.25
F_{rs}	F_{sa}	spectral shape margin	1.27	0.20
	F_d	damping margin	1.15	0.18
	F_{ssi}	soil-structure interaction	1.00	0.10
	F_m	modeling factor	1.00	0.15
	F_{mc}	modal response combination	1.00	0.05
	F_{ecc}	earthquake component combination	1.00	0.05
Overall Factor of Safety (F) and Composite Logarithmic Standard Deviation (β_c):			**9.52**	**0.44**

A_d = Ground Acceleration of the Reference Design Earthquake = 0.3 g

A_m = Median Peak Ground Acceleration = F * A_d = 9.52 * 0.3 = 2.86 g

HCLPF = A_m * exp (–2.326 * β_c) = 1.03 g

Table 15-5

Seismic Fragility for RPV Support Brackets

Component:		RPV Support Bracket		
Failure Mode:		Support		
Factor of Safety			**Median Value**	**$ß_c$**
F_c	F_s	strength margin	8.85	0.14
	F_u	inelastic energy absorption	1.00	0.00
F_{rs}	F_{sa}	spectral shape margin	1.27	0.20
	F_d	damping margin	1.08	0.12
	F_{ssi}	soil-structure interaction	1.00	0.10
	F_m	modeling factor	1.00	0.15
	F_{mc}	modal response combination	1.00	0.05
	F_{ecc}	earthquake component combination	1.00	0.05
Overall Factor of Safety (F) and Composite Logarithmic Standard Deviation ($ß_c$):			**12.14**	**0.33**

A_d = Ground Acceleration of the Reference Design Earthquake = 0.3 g

A_m = Median Peak Ground Acceleration = F * A_d = 12.14 * 0.3 = 3.64 g

HCLPF = A_m * exp (–2.326 * β_c) = 1.69 g

Table 15-6

Seismic Fragility for Control Building

Component:		Shear Walls		
Failure Mode:		Flexural		
Factor of Safety			**Median Value**	**$ß_c$**
F_c	F_s	strength margin	3.55	0.17
	F_u	inelastic energy absorption	2.65	0.25
F_{rs}	F_{sa}	spectral shape margin	1.27	0.20
	F_d	damping margin	1.15	0.15
	F_{ssi}	soil-structure interaction	1.00	0.10
	F_m	modeling factor	1.00	0.15
	F_{mc}	modal response combination	1.00	0.05
	F_{ecc}	earthquake component combination	1.00	0.05
Overall Factor of Safety (F) and Composite Logarithmic Standard Deviation ($ß_c$):			**13.73**	**0.44**

A_d = Ground Acceleration of the Reference Design Earthquake = 0.3 g

A_m = Median Peak Ground Acceleration = $F * A_d$ = 13.73 * 0.3 = 4.12 g

HCLPF = $A_m * \exp(-2.326 * \beta_c)$ = 1.48 g

Table 15-7

Seismic Fragility for Shroud Support

Component:		Shroud Support		
Failure Mode:		Buckling		
Factor of Safety			**Median Value**	**β_c**
F_c	F_s	strength margin	4.99	0.20
	F_u	inelastic energy absorption	1.00	0.00
F_{rs}	F_{sa}	spectral shape margin	1.27	0.20
	F_d	damping margin	1.08	0.12
	F_{ssi}	soil-structure interaction	1.00	0.10
	F_m	modeling factor	1.00	0.15
	F_{mc}	modal response combination	1.00	0.05
	F_{ecc}	earthquake component combination	1.00	0.05
Overall Factor of Safety (F) and Composite Logarithmic Standard Deviation (β_c):			**6.84**	**0.36**

A_d = Ground Acceleration of the Reference Design Earthquake = 0.3 g

A_m = Median Peak Ground Acceleration = F * A_d = 6.84 * 0.3 = 2.0 g

HCLPF = A_m * exp (–2.326 * β_c) = 0.87 g

Table 15-8

Seismic Fragility for CRD Guide Tubes

Component:		CRD Guide Tubes		
Failure Mode:		Buckling		
Factor of Safety			**Median Value**	**$ß_c$**
F_c	F_s	strength margin	4.16	0.20
	F_u	inelastic energy absorption	1.00	0.00
F_{rs}	F_{sa}	spectral shape margin	1.18	0.20
	F_d	damping margin	1.25	0.10
	F_{ssi}	soil-structure interaction	1.00	0.10
	F_m	modeling factor	1.00	0.15
	F_{mc}	modal response combination	1.00	0.05
	F_{ecc}	earthquake component combination	1.00	0.05
Overall Factor of Safety (F) and Composite Logarithmic Standard Deviation ($ß_c$):			**6.14**	**0.36**

A_d = Ground Acceleration of the Reference Design Earthquake = 0.3 g

A_m = Median Peak Ground Acceleration = F * A_d = 6.14 * 0.3 = 1.8 g

HCLPF = A_m * exp (–2.326 * β_c) = 0.78 g

Table 15-9

Seismic Fragility for CRD Housings

Component:		CRD Housings		
Failure Mode:		Plastic Yielding		
Factor of Safety			**Median Value**	**$ß_c$**
F_c	F_s	strength margin	7.92	0.35
	F_u	inelastic energy absorption	1.00	0.00
F_{rs}	F_{sa}	spectral shape margin	1.18	0.20
	F_d	damping margin	1.25	0.10
	F_{ssi}	soil-structure interaction	1.00	0.10
	F_m	modeling factor	1.00	0.15
	F_{mc}	modal response combination	1.00	0.05
	F_{ecc}	earthquake component combination	1.00	0.05
Overall Factor of Safety (F) and Composite Logarithmic Standard Deviation ($ß_c$):			**11.68**	**0.46**

A_d = Ground Acceleration of the Reference Design Earthquake = 0.3 g

A_m = Median Peak Ground Acceleration = F * A_d = 11.68 * 0.3 = 3.5 g

HCLPF = A_m * exp (–2.326 * β_c) = 1.2 g

Table 15-10

Seismic Fragility for Fuel Assemblies

Component:		Fuel Assemblies		
Failure Mode:		Channel Excessive Deflection		
Factor of Safety			**Median Value**	**β_c**
F_c	F_s	strength margin	2.36	0.00
	F_u	inelastic energy absorption	1.32	0.21
F_{rs}	F_{sa}	spectral shape margin	1.43	0.20
	F_d	damping margin	1.06	0.06
	F_{ssi}	soil-structure interaction	1.00	0.10
	F_m	modeling factor	1.00	0.15
	F_{mc}	modal response combination	1.00	0.05
	F_{ecc}	earthquake component combination	1.00	0.05
Overall Factor of Safety (F) and Composite Logarithmic Standard Deviation (β_c):			**4.72**	**0.35**

A_d = Ground Acceleration of the Reference Design Earthquake = 0.3 g

A_m = Median Peak Ground Acceleration = $F * A_d$ = 4.72 * 0.3 = 1.4 g

HCLPF = $A_m * \exp(-2.326 * \beta_c)$ = 0.62 g

Table 15-11

ESBWR Systems and Components/Structures Fragilities

System/Component as a function of Event Tree Node	A_m(g)	β_c	HCLPF(g)
PLANT ESS STRUCTURES (SI)			
- Reactor Building (FRBLDG)	1.90	0.45	0.67
- Containment (FCONT)	3.89	0.44	1.40
- RPV Pedestal (FPEDST)	2.86	0.44	1.03
- Control Building (FCTRBLDG)	4.12	0.44	1.48
- Reactor Pressure Vessel Support (FRPV)	3.64	0.33	1.69
DC POWER (DC)			
- Batteries (FBTR)	3.3	0.46	1.13
- Cable trays (FCTRAY)	3.0	0.60	0.74
- Motor control centers (FMCC)	1.8	0.46	0.62
REACTIVITY CONTROL SYSTEM (SCRAM)			
- Fuel assembly (FFASSY)	1.4	0.35	0.62
- CRD Guide tubes (FCRDGTB)	1.8	0.36	0.78
- Shroud support (FSHRSPT)	2.0	0.36	0.87
- CRD Housing (FCRDHS)	3.5	0.46	1.20
- Hydraulic control unit (FHYLTUT)	2.0	0.50	0.63
SRV (SRV)			
- SRV (FSRV)	3.0	0.60	0.74

Table 15-11

ESBWR Systems and Components/Structures Fragilities

System/Component as a function of Event Tree Node	A_m(g)	β_c	HCLPF(g)
STANDBY LIQUID CONTROL (SLCS)			
- Accumulator Tank (FACCT)	1.8	0.46	0.62
- Check valve (FCHV)	3.0	0.60	0.74
- Squib valve (FSQUV)	3.0	0.60	0.74
- Piping (FPIP)	3.0	0.60	0.74
- Valve (motor operated) (FMOV)	3.0	0.60	0.74
ISOLATION CONDENSER (IC)			
- Piping (FPIP)	3.0	0.60	0.74
- Heat exchanger (FICHEX)	2.0	0.45	0.70
- Valve (motor operated) (FMOV)	3.0	0.60	0.74
- Valve (nitrogen operated) (FNOV)	3.0	0.60	0.74
DPV (DPV)			
- DPV (FDPV)	3.0	0.60	0.74
GRAVITY-DRIVEN COOLING (GDCS)			
- Check valve (FCHV)	3.0	0.60	0.74
- Squib valve (FSQUV)	3.0	0.60	0.74
- Piping (FPIP)	3.0	0.60	0.74
VACUUM BREAKERS (VB)			
- Vacuum breaker valve (FVB)	3.0	0.60	0.74

Table 15-11

ESBWR Systems and Components/Structures Fragilities

System/Component as a function of Event Tree Node	A_m(g)	β_c	HCLPF(g)
PASSIVE CONTAINMENT COOLING (PCCS)			
- Heat Exchanger (FPCCSHEX)	2.0	0.45	0.70
- Piping (FPIP)	3.0	0.60	0.74
IC/PCC POOL INTERCONNECTION (PI)			
- Valve (motor operated) (FIC/PCCI)	3.0	0.60	0.74
FIRE PROTECTION WATER SYSTEM (FPW)			
- Pump (diesel driven) (FPUMPDD)	1.8	0.46	0.62

Table 15-12 Seismic Event Tree Nodal HCLPF Equations	
Top Event	**Nodal HCLPP Equations[1] [2]**
Structural Integrity (SI)	FSTRUC = FRBLDG + FCONT + FPEDST + FCTRBLDG + FRPV (0.67g + 1.40g + 1.03g + 1.48g + 1.69g = 0.67g)
DC Power (DC)	FDCP = FBTR + FCTRAY + FMCC (1.13g + 0.74g + 0.62g = 0.62g)
Scram (SCRAM)	FRC = FFASSY + FCRDGTB + FSHRSPT + FCRDHS + FHYCTUT (0.62g + 0.78g + 0.87g + 1.2g + 0.63g = 0.62g)
SRVs (SRV)	FSRV = FSRV'S = 0.74g
Standby Liquid Control (SLCS)	FSLCS = FACCT + FCHV + FSQUV + FPIP + FMOV (0.62g + 0.74g + 0.74g + 0.74g + 0.74g = 0.62g)
Isolation Condensers (IC)	FIC = FPIP + FICHEX + FMOV + FNOV (0.74g + 0.7g + 0.74g + 0.74g = 0.7g)
DPVs (DPV)	FDPV = FDPV'S = 0.74g
Gravity Driven Cooling System (GDCS)	FGDCS = FCHV + FSQUV + FPIP (0.74g + 0.74g + 0.74g = 0.74g)
Vacuum Breakers (VB)	FVB = FVB'S = 0.74g
Passive Containment Cooling (PCCS)	FPCCS = FPCCSHEX + FPIP (0.7g + 0.74g = 0.7g)
IC/PCC Pool Interconnection (PI)	FIC/PCCINT = PIC/PCCI = 0.74g
Fire Protection Water (FPW)	FFPW = FPUMPDD = 0.62g
Structural Integrity Shutdown (SIS)	FSTRUCSH = FRBLDG + FCTRBLDG + FRPV + FFASSY + FPEDST + FSHRSPT + FCONT + FCRDHS (0.67g + 1.48g + 1.69g + 0.62g + 1.03g + 0.87g + 1.4g + 1.2g = 0.62g)

Notes to Table 15-12:

(1) Refer to nodal fault trees (Figures 15-3 through 15-14) for descriptions of the individual fragility basic events.

(2) Per the MIN-MAX convention used, the overall fragility of a group of inputs combined using OR logic is determined by the lowest fragility input.

Table 15-13

HCLPF Derivation for the ESBWR Seismic Event Tree Sequences

(MIN-MAX Method)

SET Sequence	Sequence HCLPF[(1)]
Sequence 3	PI*FPW = 0.74g*0.62g = 0.74g
SEQUENCE 4	PCCS = 0.7g
Sequence 5	VB = 0.74g
Sequence 6	GDCS = 0.74g
Sequence 7	DPV = 0.74g
Sequence 8	SRV = 0.7g
Sequence 11	SCRAM*PI*FPW = 0.62g*0.74g*0.62 = 0.74g
Sequence 12	SCRAM*IC = 0.62g*0.7g = 0.7g
Sequence 13	SCRAM*SLCS = 0.62g*0.62g = 0.62g
Sequence 14	SCRAM*SRV = 0.62g*0.74g = 0.74g
Sequence 15	DC = 0.62g
Sequence 16	SI = 0.67 g

Notes to Table 15-13:

(1) Per the MIN-MAX convention used, the overall fragility of a group of inputs combined using AND logic is determined by the highest fragility input.

Table 15-14

HCLPF Derivation for the ESBWR Shutdown Seismic Event Tree Sequences

(MIN-MAX Method)

MODE 5

SET Sequence	Sequence HCLPF[(1)]
Sequence 4	IC *FPW*PI = 0.7g*0.62g*0.74g = 0.74g
Sequence 5	IC *FPW*PCCS = 0.7g*0.62g*0.7g = 0.7g
Sequence 6	IC *FPW*VB = 0.7g*0.62g*0.74g = 0.74g
Sequence 7	IC *FPW*GDCS = 0.7g*0.62g*0.74g = 0.74g
Sequence 8	IC *FPW*DPV = 0.7g *0.62g*0.74g = 0.74g
Sequence 10	IC *SRV*PIT = 0.7g *0.74g*0.74g = 0.74g
Sequence 11	IC *SRV* PCCS = 0.7g *0.74g*0.7g = 0.74g
Sequence 12	IC *SRV* VB = 0.7g*0.74g*0.74g = 0.74g
Sequence 14	IC *SRV* GDCS*PIT = 0.7g*0.74g*0.74g*0.7g = 0.74g
Sequence 15	IC* SRV* GDCS* PCCS = 0.7g*0.74g*0.74g*0.74g = 0.74g
Sequence 16	IC *SRV* GDCS* VB = 0.7g *0.74g*0.74g*0.74g = 0.74g
Sequence 17	IC *SRV* GDCS* FPW = 0.7g *0.74g*0.74g*0.62g = 0.74g
Sequence 18	IC *SRV* DPV = 0.7g*0.74g*0.74g = 0.74g
Sequence 20	IC *DC = 0.7g*0.62g = 0.7g
Sequence 21	SIS = 0.62g

MODE 6 UNFLOODED

SET Sequence	Sequence HCLPF[(1)]
Sequence 3	FPW*GDCS = 0.62g*0.74g = 0.74g
Sequence 4	DC = 0.62g
Sequence 5	SIS = 0.62g

MODE 6 FLOODED

SET Sequence	Sequence HCLPF
Sequence 2	SIS = 0.62g

Notes to Table 15-14:

(1) Per the MIN-MAX convention used, the overall fragility of a group of inputs combined using AND logic is determined by the highest fragility input.

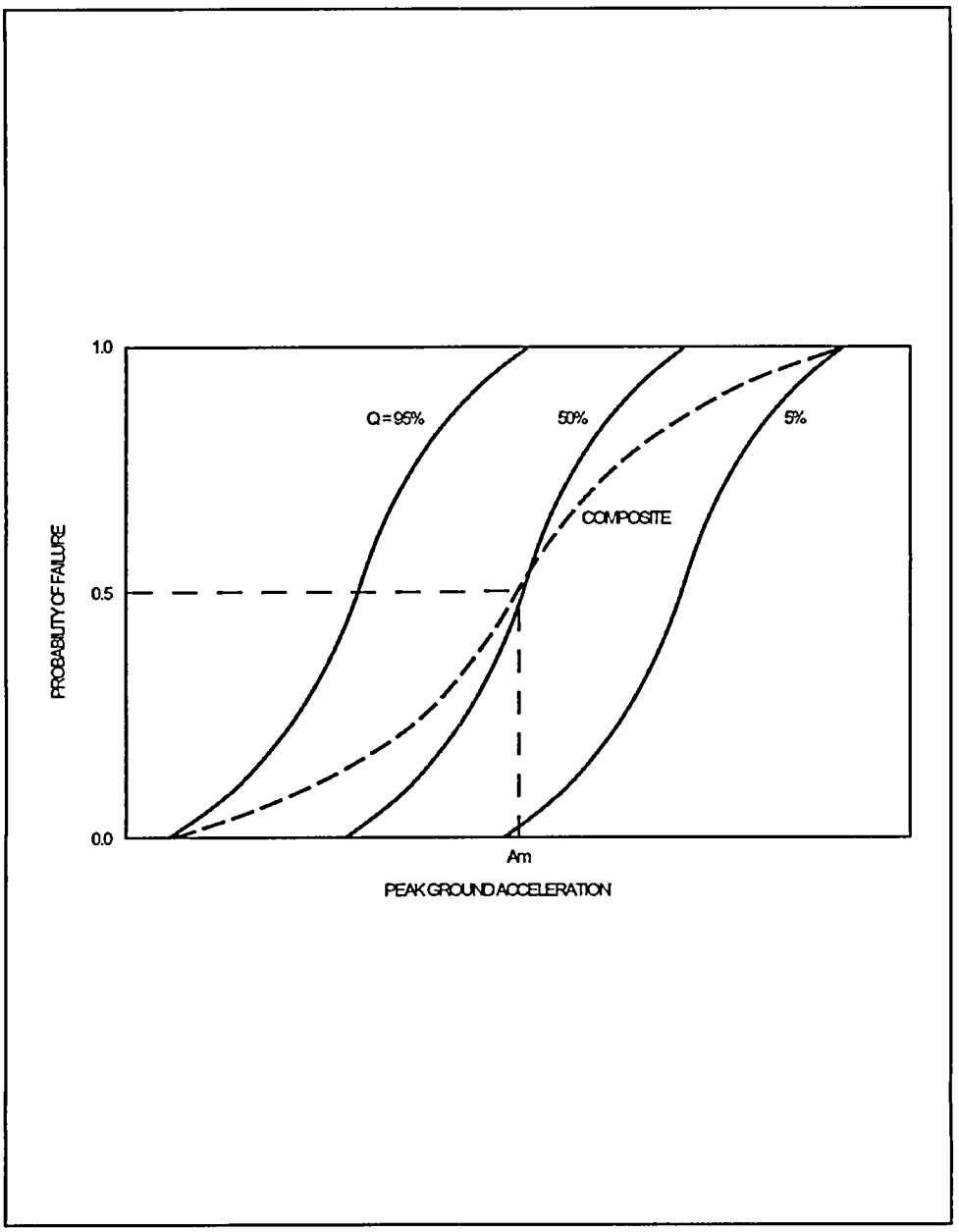

Figure 15-1. Typical Fragility Curves

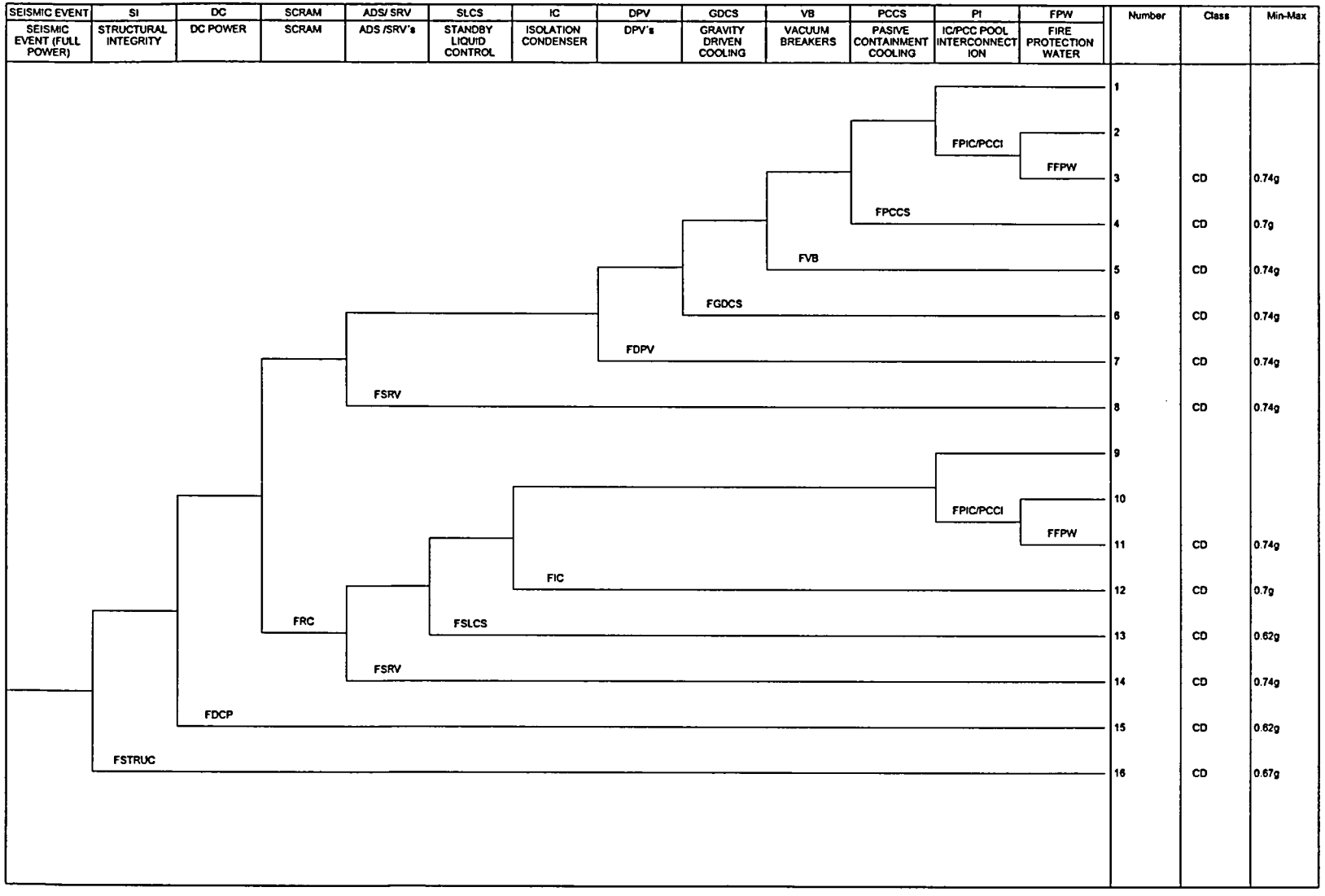

Figure 15-2. Seismic Event Tree (Full Power)

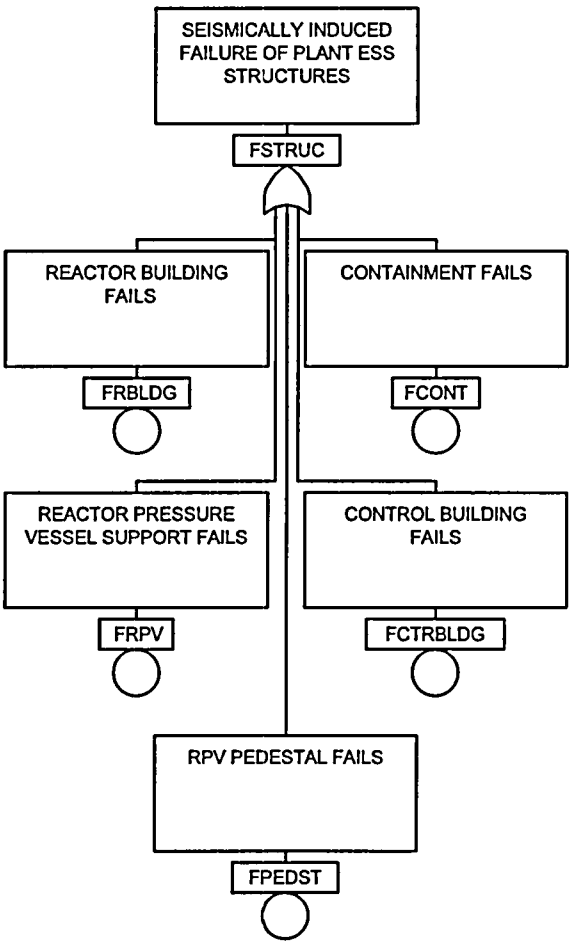

Figure 15-3. Structural Seismic Fault Tree (Full Power)

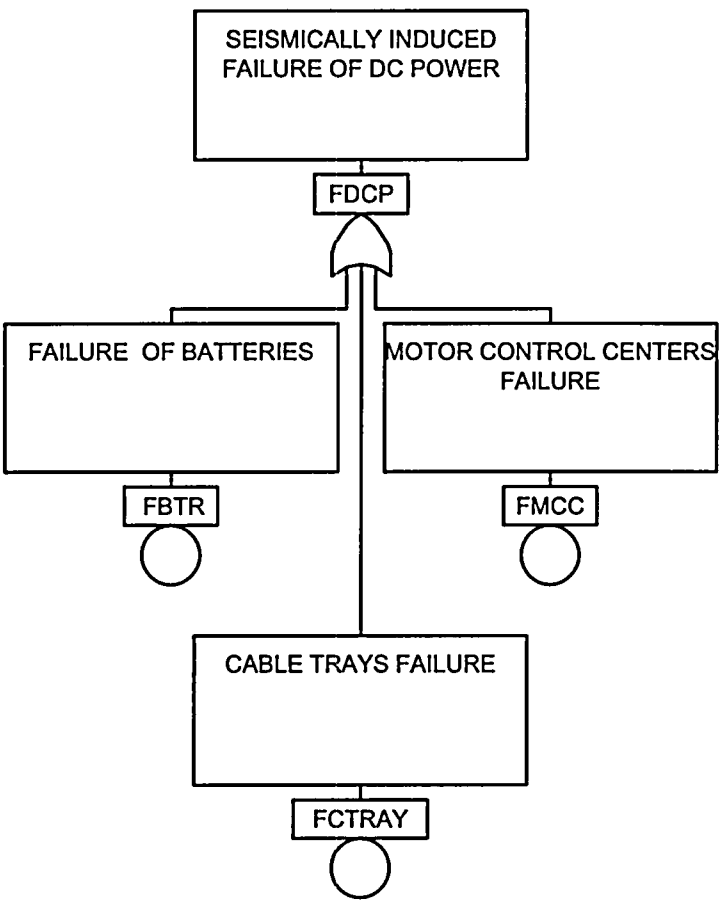

Figure 15-4. DC Power Seismic Fault Tree

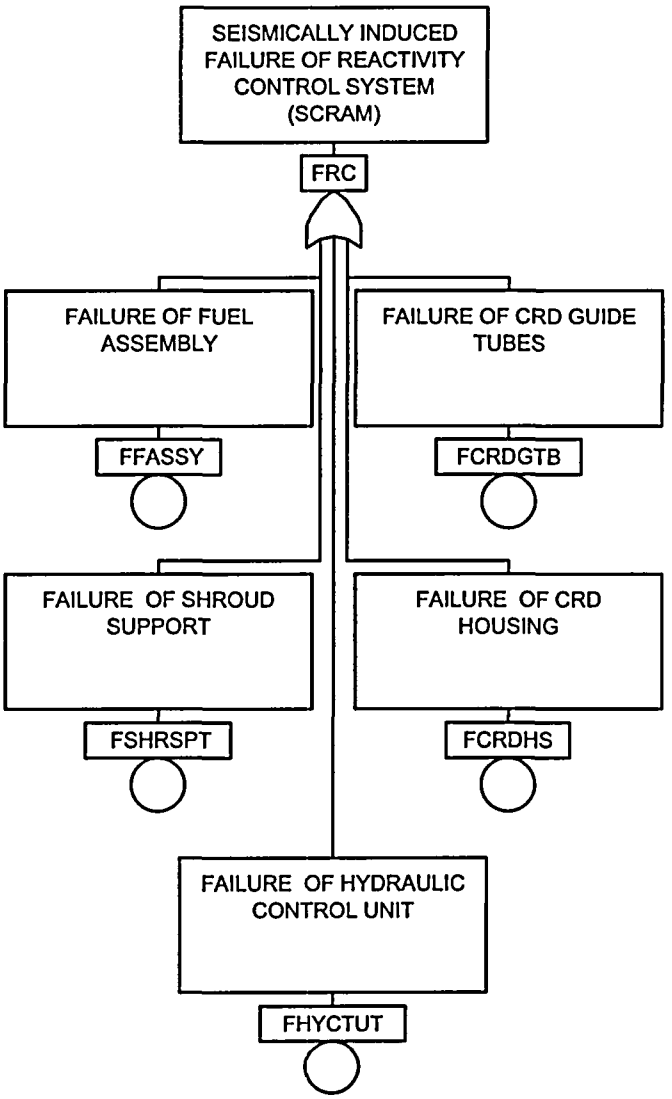

Figure 15-5. SCRAM Seismic Fault Tree

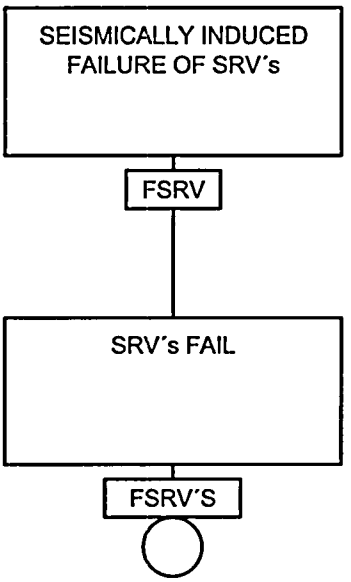

Figure 15-6. SRV Seismic Fault Tree

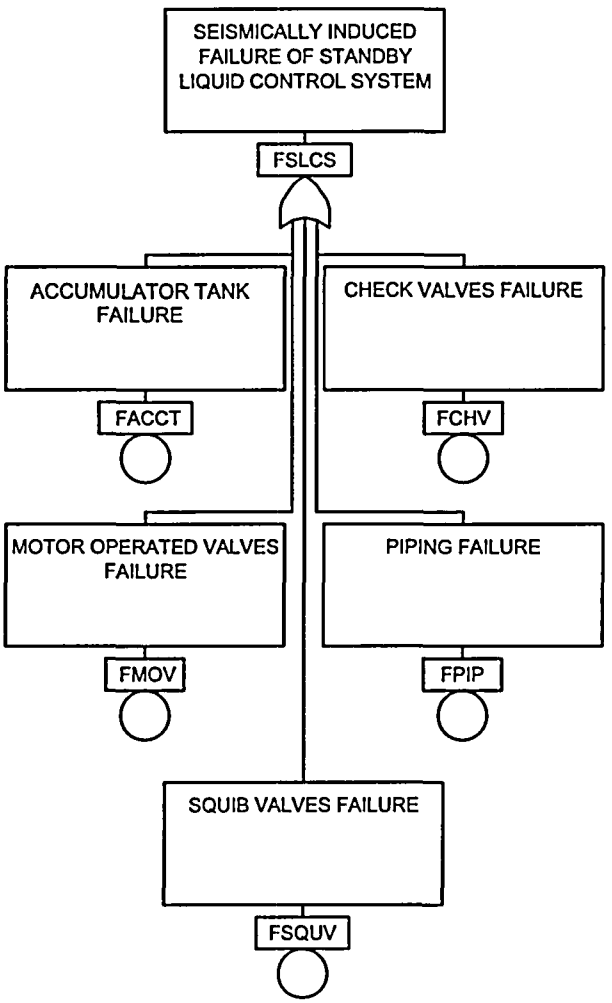

Figure 15-7. SLCS Seismic Fault Tree

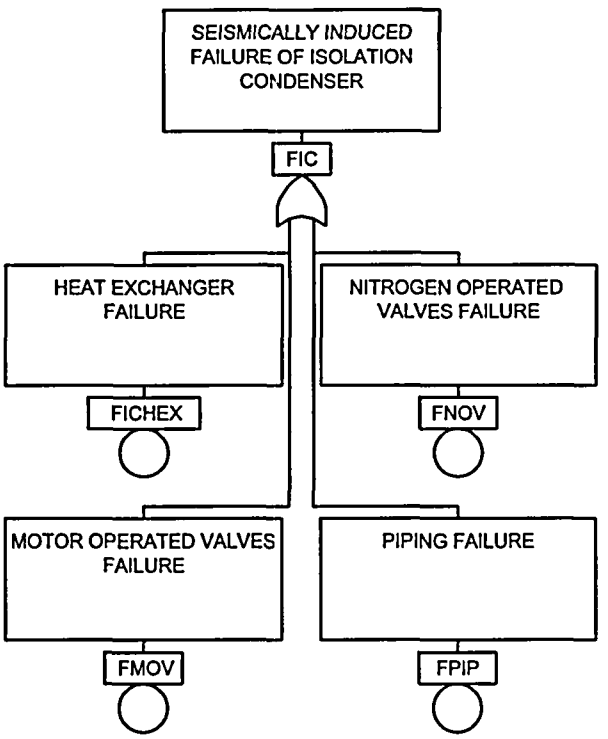

Figure 15-8. IC Seismic Fault Tree

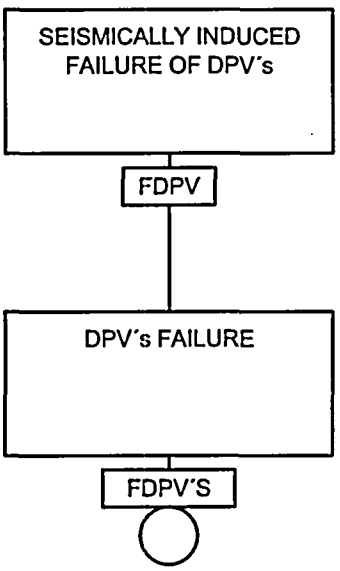

Figure 15-9. DPV Seismic Fault Tree

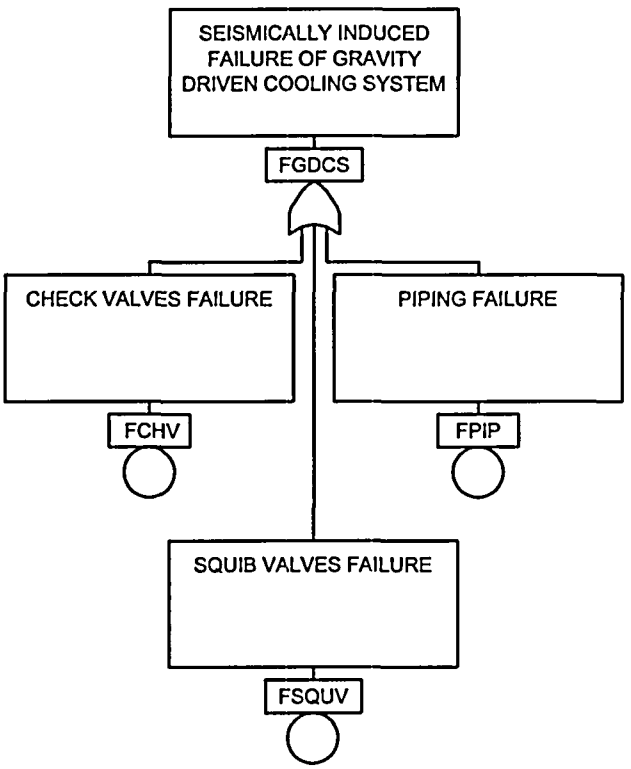

Figure 15-10. GDCS Seismic Fault Tree

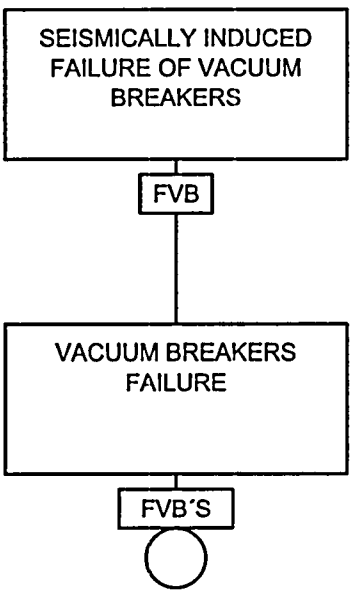

Figure 15-11. VC Seismic Fault Tree

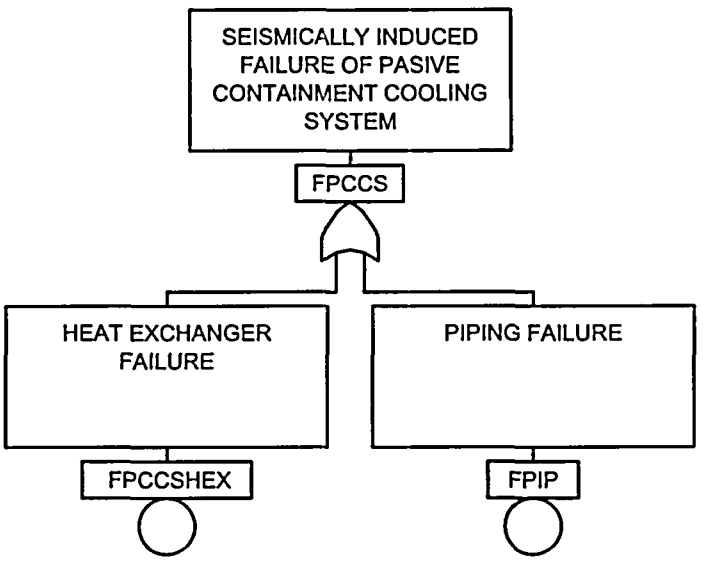

Figure 15-12. PCCS Seismic Fault Tree

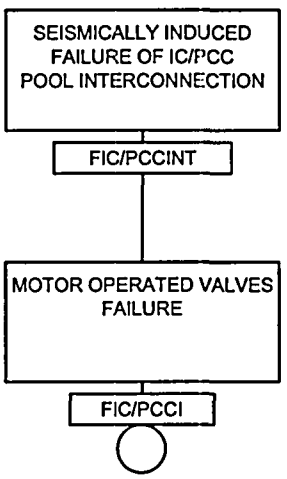

Figure 15-13. PI Seismic Fault Tree

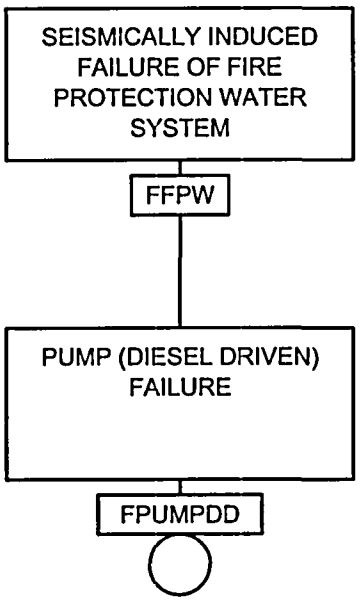

Figure 15-14. FPW Seismic Fault Tree

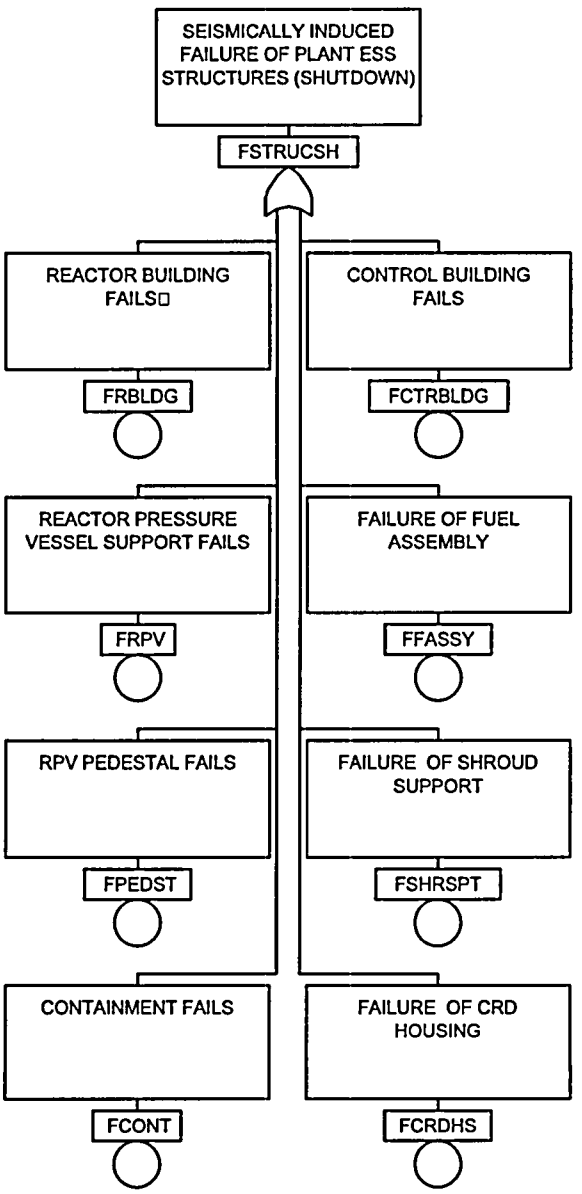

Figure 15-15. Structural Seismic Fault Tree (Shutdown Conditions)

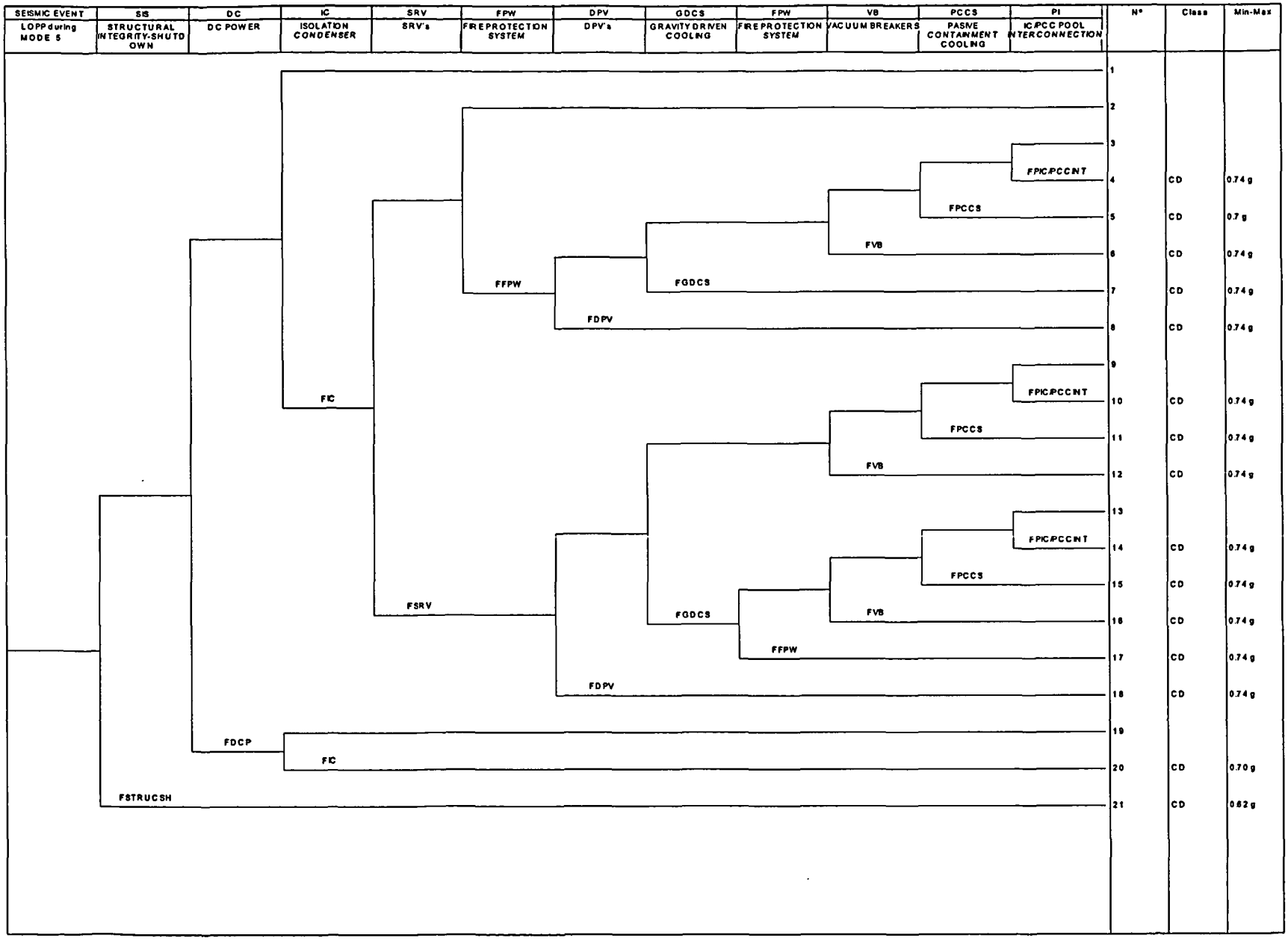

Figure 15-16. Seismic Event Tree – Shutdown Mode 5

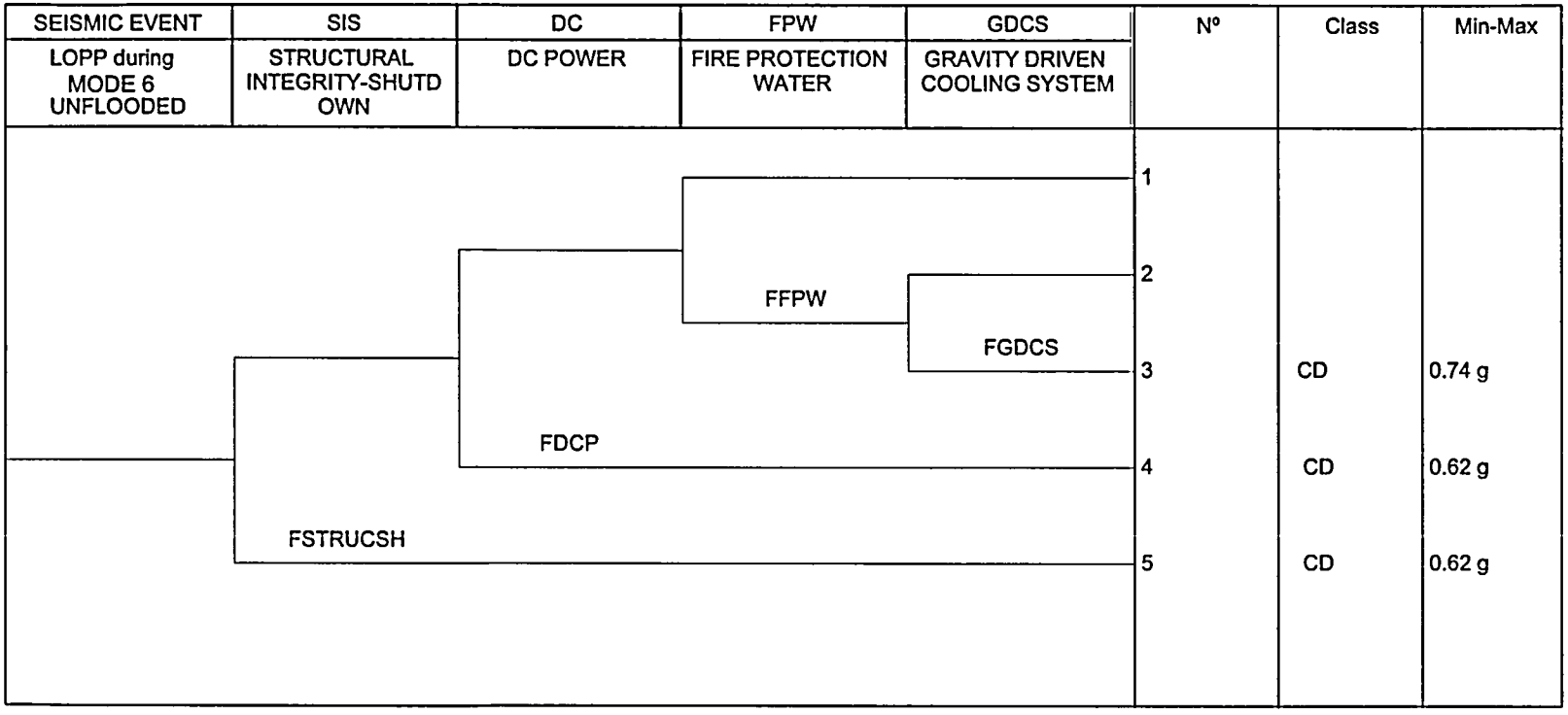

Figure 15-17. Seismic Event Tree – Shutdown Mode 6 Unflooded

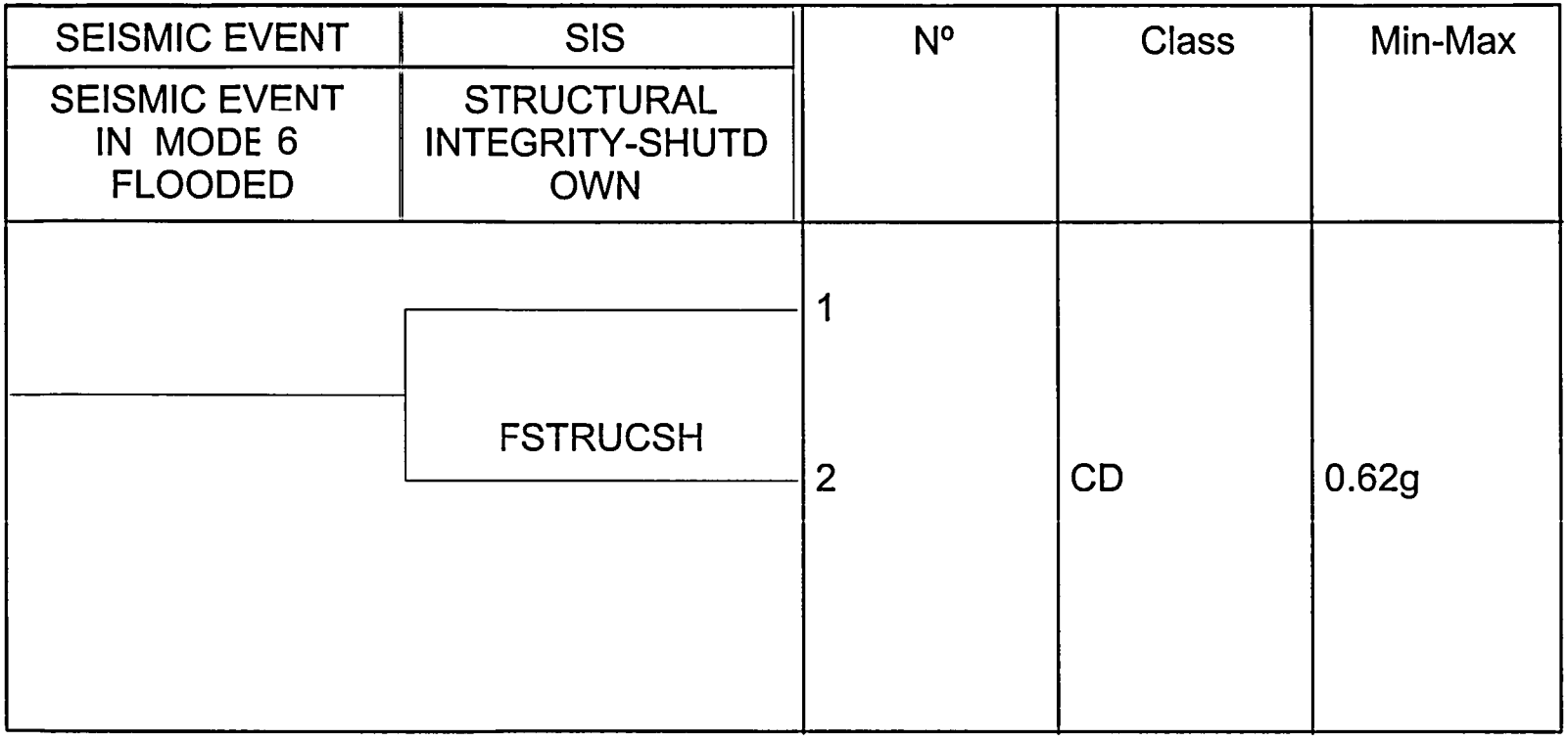

Figure 15-18. Seismic Event Tree – Shutdown Mode 6 Flooded